CHIN. PHYS. LETT. Vol. 36, No. 4 (2019) 047401

# The 0–π Phase Transition in Epitaxial NbN/$Ni_{60}Cu_{40}$/NbN Josephson Junctions *

Feng Li(李峰)[1,2,3], Wei Peng(彭炜)[1,2], Zhen Wang(王镇)[1,2,3,4]**

[1]*Shanghai Institute of Microsystem and Information Technology, Chinese Academy of Sciences, Shanghai 200050*
[2]*CAS Center for Excellence in Superconducting Electronics, Shanghai 200050*
[3]*University of Chinese Academy of Sciences, Beijing 100049*
[4]*School of Physical Science and Technology, University of ShanghaiTech, Shanghai 200031*

(Received 14 December 2018)

*We fabricate high quality superconductor/ferromagnet/superconductor (SFS) Josephson junctions using epitaxial NbN/$Ni_{60}Cu_{40}$/NbN trilayer heterostructures. Both experimental measurements and theoretical calculations of the ferromagnet layer thickness dependence of the Josephson critical current are performed. We observe the damped oscillation behavior of the critical current as a function of the ferromagnetic layer thickness at 4.2 K, which shows a 0–π phase transition in this type of magnetic Josephson junction. Clear 0–π and reverse π–0 phase transitions occur around the $Ni_{60}Cu_{40}$ thicknesses of 3.2 and 6.7 nm. Numerical calculations based on the quasi-classical Usadel equation and the Green function fit well with the experimental results. Compared with the dirty limit, the intermediate regime without the dead layer gives better fit for our SFS Josephson junctions because of the epitaxial structure. Both of the 0- and π-phase junctions show the ideal magnetic field dependence with a Fraunhofer-like pattern at 4.2 K.*

*PACS:* 74.50.+r, 85.25.Cp DOI: 10.1088/0256-307X/36/4/047401

A π-phase shift has been theoretically predicted in Josephson junctions, involving heavy-fermion superconducting systems,[1] noncentrosymmetric superconductors,[2] and cuprate superconductors.[3] The formation of π-regions in grain boundary junctions is attributed to the combined effects of the dominant $d_{x^2-y^2}$ wave order parameter symmetry of the $YBa_2Cu_3O_7$ and the faceted microstructure of the grain boundary.[4,5] By controlling the energy distribution of the current-carrying states in the normal metal, Baselmans *et al.* realized a π-junction in a superconductor/normal metal/superconductor (SNS) structure.[6] Furthermore, it has been suggested that the π-phase shift can also be observed in junctions with spin-flip scattering by magnetic impurities,[7,8] and thus realized in superconductor/ferromagnet/superconductor (SFS)[9–11] and superconductor/insulator/ferromagnet/superconductor (SIFS) Josephson junctions.[12]

Extensive investigations on the superconducting proximity effect with ferromagnets have recently uncovered some counterintuitive discoveries, such as spatial oscillations of the electron density of states,[13] a non-linear dependence of the critical temperature of S/F bilayers on the ferromagnet layer thickness[14] and the realization of π-Josephson junctions. The coexistence of superconductivity and ferromagnetism has profound implications for both fundamental physics and superconducting electronics. The size of a rapid single-flux quantum logic cell can be considerably reduced by introducing a π-junction, which is equivalent to applying a $\Phi_0/2$ flux.[15] A qubit with a π-junction circumvents the dangerous coupling to the environment through the possibility of using phase switches, rather than a permanent current bias, allowing the qubit to be manipulated.[16–18] Recently, SFS Josephson junctions have been proposed as promising candidates for cryogenic memory.[19]

In this work, we develop epitaxial NbN/$Ni_{60}Cu_{40}$/NbN structures to fabricating SFS Josephson junctions and we try to induce a critical current crossover as a function of the $Ni_{60}Cu_{40}$ thickness. In these junctions, we change the ground state by increasing the thickness $d_F$ of the ferromagnet layer. Once the phase changes from 0 to π, the value of the critical current $I_c$ becomes negative, while we can only confirm the transition with a sharp cusp in the $I_c$–$d_F$ plot because the phase measurement is rather complicated. Similarly to the coherent length $\xi_s$ in a superconductor, there is also a coherent length $\xi_F = \sqrt{\hbar D/2(\pi k_B T + iE_{ex})}$ in a ferromagnet, where $\hbar$ is the reduced Planck constant, $D$ is the diffusion coefficient for electron in the ferromagnet layer, $k_B$ is the Boltzmann constant, and $E_{ex}$ is the exchange energy of $Ni_{60}Cu_{40}$. For $E_{ex} \approx k_B T$, the decay length $\xi_{F1}$ and oscillate length $\xi_{F2}$ are given by

$$\xi_{F1,2} = \sqrt{\frac{\hbar D}{[E_{ex}^2 + (\pi k_B T)^2]^{1/2} \pm k_B T}}. \quad (1)$$

The π-phase is much more favorable when $d_F/(2\pi\xi_{F2})$ in the range of 0.4–0.8 based on the Ginzburg–Landau free-energy calculation.[9]

All of the SFS Josephson junctions reported here were fabricated in our laboratory using a process as described elsewhere.[20] The chemical stoichiometry of the $Ni_{60}Cu_{40}$ film fluctuated within a narrow range around the ratio of $Ni_{60}Cu_{40}$ target. The epitaxial NbN (200 nm)/$Ni_{60}Cu_{40}$ (2–9 nm)/NbN (200 nm) trilayer structures were continuously deposited at am-

*Supported by the Strategic Priority Research Program (A) of Chinese Academy of Sciences under Grant No XDA18000000.
**Corresponding author. Email: zwang@mail.sim.ac.cn
© 2019 Chinese Physical Society and IOP Publishing Ltd

bient temperature by magnetron sputtering on MgO (100) single crystal substrate in a high vacuum system. Figure 1 shows a cross-sectional transmission electron microscope (TEM) image of the epitaxial trilayer structure with an 8.5 nm $Ni_{60}Cu_{40}$ layer. All the junctions mentioned had dimensions of 2 μm × 2 μm.

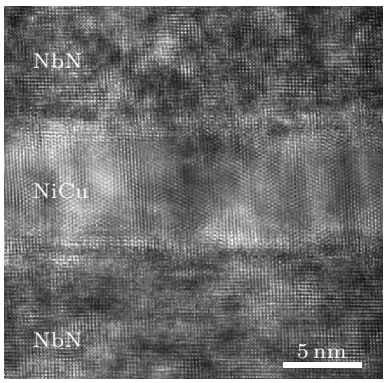


**Fig. 1.** (a) Cross-sectional TEM image of the epitaxial NbN/$Ni_{60}Cu_{40}$/NbN trilayer with an 8.5 nm $Ni_{60}Cu_{40}$ layer.

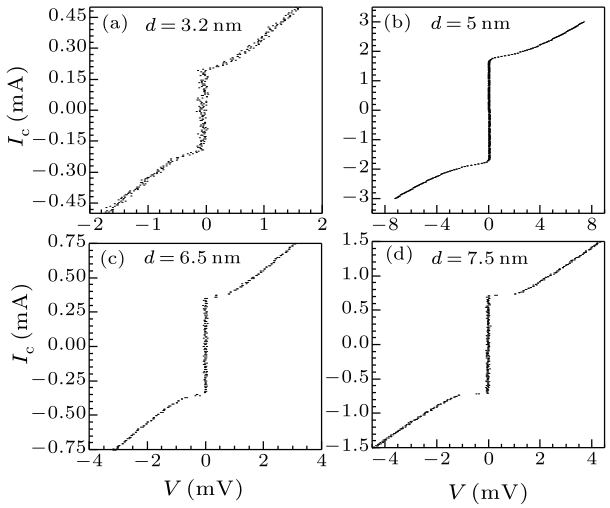


**Fig. 2.** The $I$–$V$ characteristics of SFS Josephson junction with different $Ni_{60}Cu_{40}$ thicknesses measured at 4.2 K: (a) 3.2 nm $Ni_{60}Cu_{40}$, (b) 5 nm $Ni_{60}Cu_{40}$, (c) 6.5 nm $Ni_{60}Cu_{40}$, and (d) 7.5 nm $Ni_{60}Cu_{40}$.

Figures 2(a)–2(d) show typical $I$–$V$ characteristics of 2 μm × 2 μm SFS Josephson junctions with different $Ni_{60}Cu_{40}$ thicknesses at 4.2 K. The critical current of the SFS junction with a 5-nm-thick $Ni_{60}Cu_{40}$ layer was much larger than those of the junctions with 3.2- and 6.5-nm-thick $Ni_{60}Cu_{40}$ layers. As the $Ni_{60}Cu_{40}$ thickness was increased to 7.5 nm, the critical currents of the SFS Josephson junctions increased again. The values of the normal resistance $R_n$ of those four junctions were approximately 4 mΩ, which is almost ten times as great as the resistance of the $Ni_{60}Cu_{40}$ film. Hence, the large interfacial resistance may be attributed to the atomic arrangement at the interface between NbN and $Ni_{60}Cu_{40}$ films.

The exchange energy exerted on the Cooper pair could induce a non-zero momentum center, resulting in the damped oscillation behavior of the critical current as a function of the ferromagnetic layer thickness. There are three different models in SFS Josephson junctions to explain the ferromagnet thickness dependence of the Josephson critical current, determined by the relative values of the exchange energy of the ferromagnet $E_{ex}$, the energy gap of the superconductor ($\Delta$), and $\hbar/\tau$, where $\tau$ is the mean free time between collisions of electron in the ferromagnet. The dirty limit is expressed by $\Delta \ll \hbar/\tau$ and $E_{ex} \ll \hbar/\tau$, the intermediate limit by $\Delta < \hbar/\tau$ and $E_{ex} > \hbar/\tau$, and the clean limit by $\Delta \gg \hbar/\tau$ and $E_{ex} \gg \hbar/\tau$.[21] For the simplest dirty limit, the spin-up and spin-down bands have the same Fermi velocity and mean free path. In this regime, the Usadel equation is valid for fitting the SFS Josephson junction critical current dependence on the ferromagnet thickness.[22,23]

To verify the model of our SFS Josephson junctions, we measured the resistivity of a 5-nm-thick $Ni_{60}Cu_{40}$ film by the van der Pauw technique at 4.2 K. The resistivity was $\rho_{NiCu} = 51\ \mu\Omega\cdot$cm, which is close to the value used by Weides *et al.*[24] The mean free path was calculated according to $l = m_e/\rho_F n_e e^2 = 0.21$ nm, where $m_e$ is the electron mass, $n_e$ is the carrier density, and $e$ is the electron charge. The diffusion coefficient was calculated from $D = lv_F/3 \approx 0.2\ \mathrm{cm}^2/\mathrm{s}$ with the Fermi velocity $v_F = 2.8\times10^5$ m/s.[25] The exchange energy of the 5-nm-thick $Ni_{60}Cu_{40}$ was $E_{ex} = 2\pi k_B T_c = 72$ meV, where $T_c$ is the Curie temperature of the $Ni_{60}Cu_{40}$ film. Because of $E_{ex} \gg \pi k_B T$, our epitaxial NbN based SFS junctions are in the dirty limit, and we obtained $\xi_F = \xi_{F1} = \xi_{F2} = \sqrt{\hbar D/E_{ex}} = 1.07$ nm according to Eq. (1).

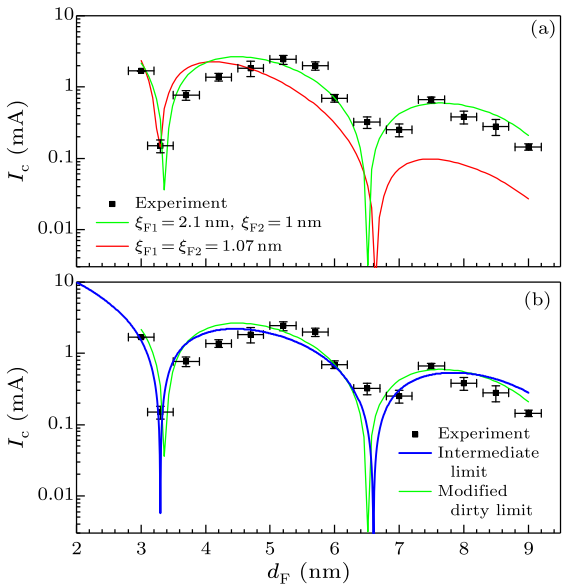


**Fig. 3.** The ferromagnet-layer thickness dependence of the critical current for NbN/$Ni_{60}Cu_{40}$/NbN junctions at 4.2 K. (a) Fitting of dirty limit with parameters $\xi_{F1} = \xi_{F2} = 1.07$ nm, $d_{dead} = 1.6$ nm and modified dirty limit with parameters $\xi_{F1} = 2.1$ nm $\xi_{F2} = 1$ nm, $d_{dead} = 1.8$ nm as shown by green and red lines, respectively. (b) Comparison between modified dirty limit and intermediate limit.

The $I_c$–$d_F$ dependence of our SFS junction was markedly non-linear, as shown in Fig. 3. Clear 0–$\pi$ and reverse $\pi$–0 phase transitions occur around the

$Ni_{60}Cu_{40}$ thicknesses of 3.2 and 6.7 nm. Each point represents a mean value with error bars showing the deviation. These local critical current minima have been observed in SFS or SIFS Josephson junctions with different ferromagnet materials and represent the phase transitions between 0-coupling and $\pi$-coupling Josephson junctions. The red line in Fig. 3(a) is fitted with the parameters $\xi_{F1} = \xi_{F2} = 1.07$ nm and $d_{dead} = 1.6$ nm according to the dirty limit regime. The dead layer may be attributed to lattice mismatch, formation of amorphous interfaces, and breakdown in the crystal structure leading to a reduced exchange interaction between neighboring atoms and a reduction in $T_{curie}$ and $E_{ex}$.[26] The phase transition occurred at $d_F^x = \frac{n\pi}{2}\xi_{F2} + d_{dead}(n = 1, 3, 5\ldots)$, while the results deviated from the model when the $Ni_{60}Cu_{40}$ layer was thicker than 6 nm. Hence, the simple dirty limit regime may not be totally suitable for our Josephson junctions. If we consider the spin-flip and spin-orbit scattering, adopt different values for the oscillation length $\xi_{F2}$ and decay length $\xi_{F1}$,[27] we can fit the $Ni_{60}Cu_{40}$ thickness dependence of the critical current with the modified dirty limit hypothesis. The green line in Fig. 3(a) is fitted by Eq. (2) with $\xi_{F1} = 2.1$ nm, $\xi_{F2} = 1$ nm, and $d_{dead} = 1.8$ nm. An equation similar to Eq. (2) has successfully been used to fit $I_c$ versus $d_F$ data for the SFS Josephson junction with $\xi_{F1} = 7.7$ nm and $\xi_{F2} = 4.4$ nm,[21]

$$I_c = I_{c0} \exp\left(\frac{-d_F}{\xi_{F1}}\right) \sin\left(\frac{d_F - d_{dead}}{\xi_{F2}} + \frac{\pi}{4}\right). \quad (2)$$

However, because of the epitaxial structure of our SFS Josephson junction, there should be no dead layer or it should be much smaller than 1.8 nm. Hence, the modified dirty limit regime is not perfect. We considered a more complicated intermediate regime to fit the experiment results. We calculated the mean free scattering time of electrons, as $\tau$ is $7.5 \times 10^{-16}$ s with $l$ and $v_F$. The value of $E_{ex}\tau$ $(5.5 \times 10^{-14})$ is larger than $\hbar$ $(4.1 \times 10^{-15})$ while $\Delta\tau$ $(2.1 \times 10^{-15})$ is smaller than $\hbar$, which indicates that the intermediate limit may also be suitable.

The value of $I_c$ is

$$I_c(d_F) \propto \pi T \sum_{n \geqslant 0} \frac{\Delta^2}{\Delta^2 + \omega_n^2} \frac{\sin(d_F/\xi_{F2})}{d_F/\xi_{F2}} \cdot \exp\left[\frac{-d_F}{\xi_{F1}}(1 + 2\omega_n\tau)\right], \quad (3)$$

where $\omega_n = \pi k_B T(2n + 1)$ is the Matsubara frequency, and $n$ is an integer. By fitting our data with Eq. (3),[28] we obtain the parameters $\xi_{F1} = 4$ nm, $\xi_{F2} = 1.05$ nm, without any dead layer. The blue line in Fig. 3(b) is fitted by the intermediate regime, whereas the green line was fitted with the modified dirty limit. Comparing these two equations, the values of $\xi_{F2}$ were quite close, whereas $\xi_{F1}$ was somewhat larger in intermediate regime, which is consistent with the effects of weak magnetic scattering. No dead layer was taken into consideration because of the epitaxial nature of the structure. In Table 1 we give an overview on SFS Josephson junction parameters compared with that in other groups.

**Table 1.** Summary of junction parameters of the SFS and SIFS Josephson junctions reported for different material systems. DL is the dead layer thickness.

| Ferromagnet | Structure | $\xi_{F1}$ (nm) | $\xi_{F2}$ (nm) | DL (nm) | $E_{ex}$ (meV) | $v_F$ (m/s) | |
|---|---|---|---|---|---|---|---|
| $Ni_{60}Cu_{40}$ | SFS | 4 | 1.05 | | 85 | $2.8 \times 10^5$ | This work |
| $Ni_{53}Cu_{47}$ | SFS | 1.3 | 3.5 | | 73 | | Ref. [10] |
| $Ni_{60}Cu_{40}$ | SIFS | 0.78 | 1.35 | 3.09 | 99 | $2.8 \times 10^5$ | Ref. [12] |
| $Ni_{80}Fe_{20}$ | SFS | 1.4 | 0.46 | 0.5 | 201 | $2.2 \times 10^5$ | Ref. [29] |
| $Ni_{80}Fe_{20}$ | SFS | 1.2 | 1.6 | 0.7 | 95 | $2.2 \times 10^5$ | Ref. [30] |

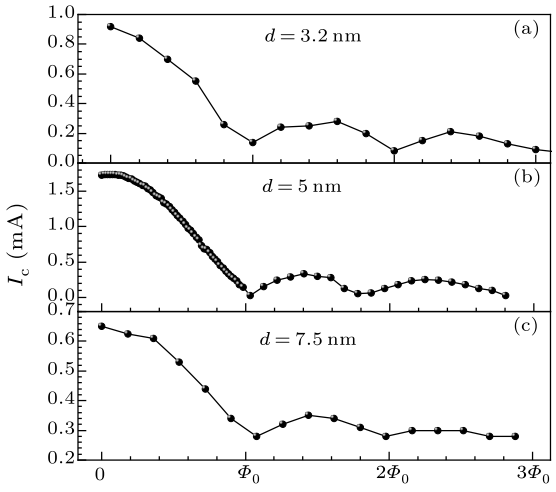


**Fig. 4.** Critical current versus magnetic field of junctions with 3.2, 5, and 7.5 nm $Ni_{60}Cu_{40}$.

The magnetic-field dependence of the critical currents at 4.2 K is shown in Fig. 4 for 3.2-, 5-, and 7.5-nm-thick $Ni_{60}Cu_{40}$ Josephson junctions at $\pi$- or 0-phase states. It is difficult to confirm the phase state of the 3.2 nm junction, which lies around the phase transition position. The critical currents decreased to near zero when the magnetic flux $\Phi = n\Phi_0$ ($n$ is an integer). The residual current may be related to the higher harmonic current-phase relation or quasiparticle current, which will be clarified in our future studies.

In summary, both 0–$\pi$ and $\pi$–0 phase transitions have been observed in epitaxial NbN/$Ni_{60}Cu_{40}$/NbN Josephson junctions. The damping length $\xi_{F1}$ and oscillation length $\xi_{F2}$, as calculated for the $Ni_{60}Cu_{40}$ material, are close to those used in fitting of the experimental results for 0–$\pi$ phase transition dependence on $Ni_{60}Cu_{40}$ thickness. The intermediate regime without a dead layer gives better fit for our SFS Josephson junctions because of the epitaxial structure. When the thickness of $Ni_{60}Cu_{40}$ is approximately 3.2 nm,

the junction transforms from the 0-state to the $\pi$-state and switches back from the $\pi$-state to the 0-state at approximately 6.7 nm. Both the 0-phase (7.5-nm-thick $Ni_{60}Cu_{40}$) and $\pi$-phase (5-nm-thick $Ni_{60}Cu_{40}$) SFS Josephson junctions show ideal magnetic field dependences.

## References


[1] Geshkenbein V B and Larkin A I 1986 *JETP Lett.* **43** 395
[2] Liu J F, Zhang H and Wang J 2016 *Chin. Phys. B* **25** 097403
[3] Sigrist M and Rice T M 1992 *J. Phys. Soc. Jpn.* **61** 4283
[4] Hilgenkamp H, Mannhart J and Mayer B 1996 *Phys. Rev. B* **53** 14586
[5] Smilde H J H, Ariando, Blank D H A, Gerritsma G J, Hilgenkamp H and Rogalla H 2002 *Phys. Rev. Lett.* **88** 057004
[6] Baselmans J J A, Morpurgo A F, van Wees B J and Klapwijk T M 1999 *Nature* **397** 43
[7] Bulaevskii L N, Kuzii V V and Sobyanin A A 1977 *JETP Lett.* **25** 290
[8] Peng L, Liu Y S, Cai C B and Zhang J C 2011 *Chin. Phys. Lett.* **28** 087401
[9] Ryazanov V V, Oboznov V A, Rusanov A Y, Veretennikov A V, Golubov A A and Aarts J 2001 *Phys. Rev. Lett.* **86** 2427
[10] Oboznov V A, Bol'ginov V V, Feofanov A K, Ryazanov V V and Buzdin A I 2006 *Phys. Rev. Lett.* **96** 197003
[11] Yamashita T, Kawakami A and Terai H 2017 *Phys. Rev. Appl.* **8** 054028
[12] Weides M, Kemmler M, Kohlstedt H, Waser R, Koelle D, Kleiner R and Goldobin E 2006 *Phys. Rev. Lett.* **97** 247001
[13] Pepe G P, Latempa R, Parlato L, Ruotolo A, Ausanio G, Peluso G, Barone A, Golubov A A, Fominov Y V and Kupriyanov M Y 2006 *Phys. Rev. B* **73** 054506
[14] Fominov Y V, Chtchelkatchev N M and Golubov A A 2002 *Phys. Rev. B* **66** 014507
[15] Ustinov A V and Kaplunenko V K 2003 *J. Appl. Phys.* **94** 5405
[16] Ioffe L B, Geshkenbein V B, Feigel'man M V, Fauchere A L and Blatter G 1999 *Nature* **398** 679
[17] Yamashita T, Tanikawa K, Takahashi S and Maekawa S 2005 *Phys. Rev. Lett.* **95** 097001
[18] Blatter G, Geshkenbein V B and Ioffe L B 2001 *Phys. Rev. B* **63** 174511
[19] Ryazanov V V, Bol'ginov V V, Sobanin D S, Vernik I V, Tolpygo S K, Kadin A M and Mukhanov O A 2012 *Phys. Procedia* **36** 35
[20] Li F, Zhang H, Zhang L, Peng W and Wang Z 2018 *AIP Adv.* **8** 055007
[21] Khaire T S, Pratt W P and Birge N O 2009 *Phys. Rev. B* **79** 094523
[22] Usadel K D 1970 *Phys. Rev. Lett.* **25** 507
[23] Buzdin A I, Vujicic B and Kupriyanov M Y 1992 *Zh. Eksp. Teor. Fiz.* **101** 231
[24] Weides M, Kemmler M, Goldobin E, Koelle D, Kleiner R, Kohlstedt H and Buzdin A 2006 *Appl. Phys. Lett.* **89** 122511
[25] Petrovykh D Y, Altmann K N, Hochst H, Laubscher M, Maat S, Mankey G J and Himpsel F J 1998 *Appl. Phys. Lett.* **73** 3459
[26] Aarts J, Geers J M E, Bruck E, Golubov A A and Coehoorn R 1997 *Phys. Rev. B* **56** 2779
[27] Faure M, Buzdin A I, Golubov A A and Kupriyanov M Y 2006 *Phys. Rev. B* **73** 064505
[28] Bergeret F S, Volkov A F and Efetov K B 2001 *Phys. Rev. B* **64** 134506
[29] Robinson J W A, Piano S, Burnell G, Bell C and Blamire M G 2006 *Phys. Rev. Lett.* **97** 177003
[30] Bell C, Loloee R, Burnell G and Blamire M G 2005 *Phys. Rev. B* **71** 180501